

Imaging and tracking of single hyaluronan molecules diffusing in solution

Tim Kaminski · Jan-Peter Siebrasse ·
Volkmar Gieselmann · Ulrich Kubitscheck ·
Joachim Kappler

Received: 2 November 2007 / Revised: 14 January 2008 / Accepted: 16 January 2008 / Published online: 8 February 2008
© Springer Science + Business Media, LLC 2008

Abstract Hyaluronan is an important soluble component of the extracellular matrix of many tissues with well known space-filling, lubricating and signaling functions. As such, hyaluronan can regulate cell adhesion, migration, differentiation and proliferation. Ultrastructural studies showed the existence of fibers and networks of hyaluronan molecules at surfaces, while bulk studies of hyaluronan in solution indicated that the polymer forms random coils. Here, we show that single hyaluronan molecules can be visualized and tracked in three-dimensional samples at room temperature in aqueous buffer. Using a wide-field fluorescence microscope equipped with laser excitation and an sensitive and fast EMCCD camera for fluorescence detection, single FITC-labeled hyaluronan molecules from rooster comb were detected in aqueous solutions. Freely moving hyaluronan-FITC could be tracked over up to 20 images acquired at a frame rate of 98 Hz. Analysis of the trajectories revealed Brownian motion of hyaluronan in tris-buffered saline with an average diffusion coefficient $D=3.0\pm 0.2 \mu\text{m}^2/\text{s}$. These observations confirm the concept that hyaluronan molecules form random coils in solution. The possibility of following

the tracks of single hyaluronan molecules in solution facilitates the analysis of processes that lead to the formation of more organized forms of hyaluronan and its interactions with cells with very high spatial and temporal accuracy.

Keywords Hyaluronan · Single molecule microscopy · Biophysics

Introduction

Hyaluronan is a free glycosaminoglycan, which is abundant in the extracellular matrix of many tissues including skin, vessels, cartilage and brain. This unbranched glycosaminoglycan is formed from GlcUA β 1-3GlcNAc building blocks linked together by β 1-4 glycosidic linkages. It can reach a size of 20,000 kDa (for review [18] and references cited therein). Despite its simple structure, the hyaluronan polymer has a wide range of important biological functions, which are size- and presumably conformation-dependent (reviewed in [4, 23]). These functions include enhancement of cell migration (*e.g.* during neural crest cell development or in tumor cells), regulation of cell proliferation, and control of angiogenesis. Furthermore, hyaluronan influences cell differentiation, immune responses and wound repair [23].

The wide range of biological functions of hyaluronan suggested the existence of a correspondingly large repertoire of hyaluronan sizes and conformations with specific binding interactions [4]. However, extensive rheological studies of the viscoelastic properties of hyaluronan failed to reveal stable conformations of this polymer in solution [4]. Instead, hyaluronan seems to form random coils in solution filling huge hydrodynamic volumes and simple transient intermolecular interactions seem to determine the viscosity of hyaluronan solutions [4]. A detailed study by Gribbon *et al.*

Electronic supplementary material The online version of this article (doi:10.1007/s10719-008-9112-1) contains supplementary material, which is available to authorized users.

T. Kaminski · V. Gieselmann · J. Kappler (✉)
Institut für Physiologische Chemie,
Rheinische Friedrich-Wilhelms-Universität Bonn,
Nussallee 11,
53115 Bonn, Germany
e-mail: kappler@institut.physiochem.uni-bonn.de

J.-P. Siebrasse · U. Kubitscheck
Institut für Physikalische und Theoretische Chemie,
Rheinische Friedrich-Wilhelms-Universität Bonn,
Wegelerstraße 12,
53115 Bonn, Germany

[11] using fluorescence recovery after photobleaching (FRAP) with a confocal microscope on a minute timescale provided analyses of the dependence of the diffusion coefficient of hyaluronan on concentration, solution composition and temperature. The results of this study are in agreement with the concept that hyaluronan forms random coils in solution. These conclusions from bulk measurements in solution contrast with the picture, which emerges from the visualization of single hyaluronan molecules at high spatial resolution on mica surfaces. Rotatory shadowing electron microscopy showed organization of hyaluronan into branched networks [20]. Similarly, atomic force microscopy revealed extended and condensed forms of hyaluronan, which also formed networks and twisted fibers [5]. Interestingly, in tissues more organized fiber- or cable-like hyaluronan-structures have been reported [2, 9].

There seem to be at least two possible explanations for the fact that ultrastructural studies of hyaluronan molecules fail to reveal random coil structures, but indicate the presence of more organized forms. First, hyaluronan may form organized structures in solution which are highly dynamic and thus can escape detection in studies where the time resolution of the method is not sufficient. Secondly, random coils of hyaluronan may form only in solution, while interaction of the polymer with surfaces may induce organization into networks or fibers. As a first step of distinguishing between these possibilities it is necessary to visualize single hyaluronan molecules at high temporal and spatial resolution as they move freely in solution. In the present study we use highly sensitive fast fluorescence microscopy on a millisecond scale to examine the solution shape and mobility of single hyaluronan molecules from rooster comb after labeling with FITC.

Materials and methods

Preparation and biochemical characterization of FITC-labeled hyaluronan Hyaluronan from rooster comb (Sigma Cat. H5388) was labelled with fluorescein isothiocyanate (FITC; Fluka, Cat. 46950) [7]. Briefly, hyaluronan (0.1 g) was dissolved in formamide (5 mg/ml) for 48 h and the residue was filtered off on a G-2 glass filter. To 1 ml filtrate dimethylsulfoxide (1 ml) was added together with sodium hydrogen carbonate (2.5 mg), dibutyltin dilaurate (2.5 mg), and FITC (6 mg), and the reaction mixture was stirred on a steam bath for 30 min. The product was diluted with water and precipitated repeatedly ($n \approx 10$) in ethanol until the product was free from non-bound label. Hyaluronan was quantified using the carbazol method [3]. For calibration a hyaluronan dilution series (0.4–500 $\mu\text{g/ml}$) was used. The concentration of fluorophores was determined fluorometrically (Genios, Tecan) by comparison with a FITC calibration curve. The

size distribution of the hyaluronan was determined by agarose gel electrophoresis using a BstEII digest of lambda DNA as marker (Fermentas, St. Leon-Rot, Germany) [16]. Comparison of the mobilities of hyaluronan samples of known size and the marker bands showed that the mobility 1 bp of DNA corresponded to 170 Da of hyaluronan (accordingly, the marker band with a size of 14,140 bp corresponded to a hyaluronan size of 2.4 MDa).

Data acquisition Single-particle tracking (SPT) experiments were performed using a custom-built single-molecule microscope based on a Zeiss Axiovert 200TV equipped with an $\times 63$ NA 1.4 oil immersion objective lens (Carl Zeiss Microimaging GmbH, Jena, Germany) [21]. FITC fluorescence was excited at 488 nm by a diode pumped solid-state laser (Sapphire 488-100, Coherent Inc., Santa Clara, CA, USA). Laser illumination was switched on only during image acquisition by means of an acousto-optical tunable filter. For single-particle image acquisition we used the iXon DV 860 BI camera (Andor Technology, Belfast, Northern Ireland) in combination with a $\times 4$ magnifier yielding a pixel size in the object space of 95.24 nm. Generally, 30 frames were recorded in a single movie, with an integration time 10 ms and a frame rate of $k_{\text{acq}} = 97.85$ Hz.

Image processing of video images Identification and tracking of the single-molecule signals was accomplished using Diatrack 3.0 (Semaphot, North Epping, Australia), a commercial image processing program for the identification and localization of single-particle signals and trajectories as described [13]. For tracking a maximal displacement of ten pixels from frame to frame was allowed. After processing with Diatrack we verified the single-particle trajectories in the original, unprocessed data by visual inspection.

Trajectory analysis Each FITC hyaluronan trajectory was defined as a set of coordinates (x_i, y_i) with $1 < i < N$, where N denoted the total number of observations. These paths were plotted and overlaid. In the case of two-dimensional Brownian motion the mean square displacements, $\langle r^2(t_c) \rangle$ are related to time and diffusion coefficient, D :

$$\langle r^2(t_c) \rangle = 4Dt_c. \quad (1)$$

The mean square displacement was plotted against time and the data fitted using weighted linear regression analysis (Origin 6.1 software). The probability that a particle starting at a specific position will be encountered within a shell of radius, r , and width, dr , at time, t , from that position is for a single species diffusing in two dimensions given as follows [6]:

$$p(r, t)dr = (4\pi Dt)^{-1} e^{-r^2/4Dt} 2\pi r dr \quad (2)$$

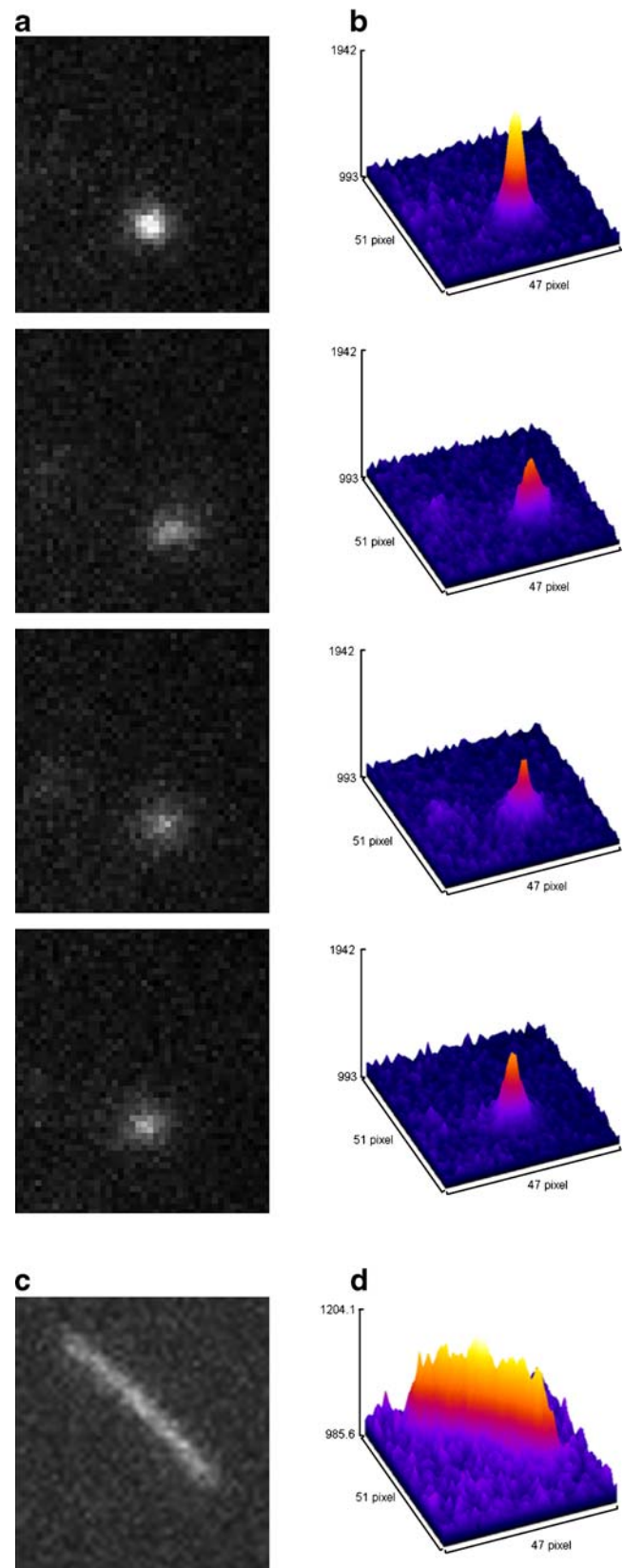
if we identify the starting position with the origin. Experimentally, this probability distribution could be approximated by a frequency distribution, which was obtained by counting the jump distances within respective intervals $[r, r + dr]$ traveled by single particles after a given time lag.

Results and discussion

When hyaluronan from rooster comb was labeled with FITC a degree of labeling of 0.4% of the disaccharide units was determined (data not shown). The degree of labeling determined in the present study was in agreement with the literature [7]. Since more than 99% of the disaccharide units were left unmodified a gross alteration of the global conformation of labeled hyaluronan chains seemed unlikely. The average mass of hyaluronan-FITC was 1,500 kDa as determined by agarose gel electrophoresis (Supplementary material). Thus, on average 15 fluorophores were present per molecule.

Using wide field excitation images of single hyaluronan were acquired in the three-dimensionally extended sample in physiological saline buffered with tris (2-amino-2-(hydroxymethyl)propane-1,3-diol). Figure 1 shows a raw image sequence of a sample with the objective lens focused on a plane inside the sample volume without any further background manipulation or filtering. Images were recorded with an integration time of 10 ms with a cycle time of 97.85 Hz. Distinct fluorescence maxima corresponded to the positions of a single hyaluronan molecule. In all experiments highly diluted samples of hyaluronan-FITC with a final concentration of ≈ 300 pM in aqueous buffer without any additives, which might increase the viscosity of the solution, were used. In these images there was no indication of the formation of ordered arrays of hyaluronan or the presence of extended rod-like molecular shapes, which would indicate the presence of organized hyaluronan forms. Sharply focussed images showed round intensity spots as expected for a polymer forming a spherical random coil, and had a FWHM diameter of 367 nm ($n=41$). Because each disaccharide building block has a length of approx. 1 nm a hyaluronan molecule with a mass of 1.5 MDa has a predicted contour length of about 4 μm . In contrast to the small size and the round

Fig. 1 Movements of a hyaluronan-FITC molecule in solution. **a** Sequence of consecutive raw images. **b** Surface plots of the raw image. The object field size shown is $4.5 \times 4.5 \mu\text{m}^2$. Images were taken with an integration time of 10 ms at a frame rate of 97.85 Hz. **c** For comparison, an image of an actin filament with a contour length of approximately 4 μm is shown. **d** Surface plot of the actin filament raw image shown in **c**. Bar, 1 μm



appearance of hyaluronan molecules, a single actin microfilament of comparable contour length had clearly an extended shape, when it was visualized after labeling with phalloidin-TRITC with our microscopic setup (Fig. 1c). There was also no indication of more organized forms of hyaluronan, when the lower glass surface of the sample chamber was brought into focus. Thus, the images recorded from single hyaluronan molecules at high dilution in solution were consistent with the concept that they form random coils of approximately spherical shape (Fig. 1). This finding was in agreement with the conclusions drawn from viscometric studies (reviewed in [4]) and from FRAP experiments [11].

From the image sequences sets of space–time coordinates $\{x(t_i), y(t_i), t_i\}$ were derived after fitting of filtered and background subtracted signals with 2D-Gaussian functions, which were employed to approximate the diffraction-limited signals. These sets represented 2D projections of their 3D trajectories. Taken together, 1,920 images in 64 sequences were analyzed containing 144 detected trajectories. Figure 2 shows an overlay of all trajectories. These paths did not display any directional bias suggesting that the observed two dimensional projections of the trajectories to the horizontal focus plane reflected a purely diffusive lateral motion of hyaluronan-FITC.

To confirm diffusive transport of hyaluronan-FITC molecules the mean square displacement was examined over time. A linear relationship between $r^2(t_c)$ and time indicates Brownian (diffusive) motion. A plot of the average

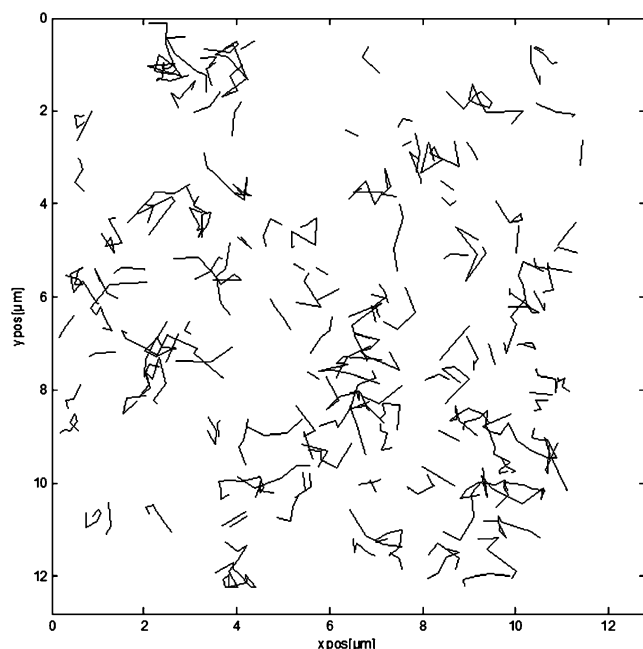


Fig. 2 Overlay of trajectories of single hyaluronan-FITC molecules. The 144 trajectories obtained by single molecule microscopy at 97.85 Hz and tracking with Diatrack were plotted into the same diagram. The field size shown is $12.2 \times 12.2 \mu\text{m}^2$

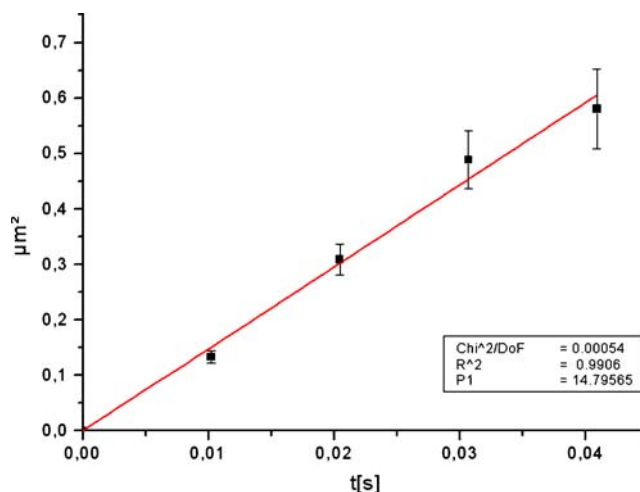


Fig. 3 Linear dependence of mean square displacements of hyaluronan-FITC molecules as a function of time. All measurements were performed at a temperature of 22°C . Filled squares represent mean values of the mean square displacement [for each frame number the corresponding n is given in brackets: 1 (144), 2 (122), 3 (97), 4 (69)]. Error bars represent the SEM. The red line represents a linear fit of the mean values through the origin

mean square displacement over time is shown in Fig. 3. The mean square displacement increased linearly with time. Based on this analysis of the projections of trajectories to the focus plane we conclude that there is no evidence for convective transport in x - or y -direction. Thus, the mean square displacement plot over time was used to estimate the average diffusion coefficient of hyaluronan-FITC according to the equation $r^2(t_c) = 4D_{\text{msd}}t_c$. Linear regression analysis yielded $D_{\text{msd}} = 3.7 \pm 0.1 \mu\text{m}^2/\text{s}$ with $R^2 = 0.9906$.

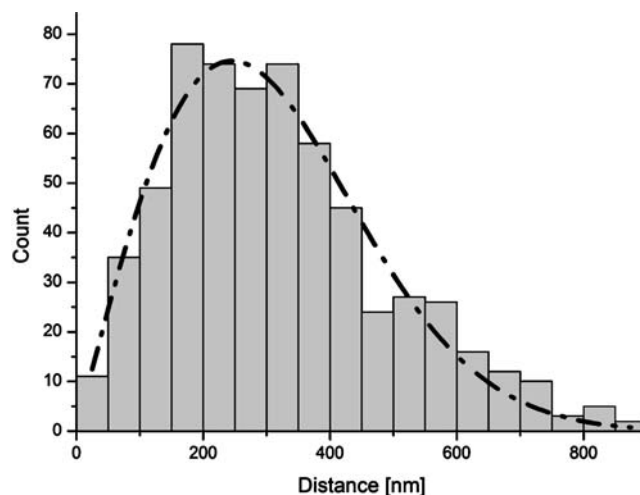


Fig. 4 Hyaluronan-FITC mobility in solution. Jump distance distribution for all single hyaluronan-FITC molecules, which were identified and tracked in the movies acquired at 97.85 Hz. Filled bars represent the frequencies of jumps in the different classes as indicated at the x axis. The dashed line represents the best fit of the data using a model assuming a single diffusing species of hyaluronan. $D = 3 \pm 0.2 \mu\text{m}^2/\text{s}$ was obtained

As an independent computational approach to determine the average diffusion coefficient of hyaluronan from rooster comb, and to check for possibly aggregated molecules causing an additional mobility fraction, we analyzed the distribution of all jump distances in all trajectories ($n=618$ jumps; Fig. 4). Fitting of this distribution with a model assuming a single diffusing species yielded a satisfactory description of the data, and an average diffusion coefficient of $D_{jd}=3.0\pm 0.2 \mu\text{m}^2/\text{s}$ (Fig. 4). This value was only slightly smaller than the diffusion coefficient measured from the mean square distance analysis.

Our data confirm the Brownian motion of hyaluronan from rooster comb (molecular weight 1,500 kDa) with an average diffusion coefficient $D=3 \mu\text{m}^2/\text{s}$ based on the jump distance (Fig. 4). Our hyaluronan diffusion coefficient in the presence of physiological concentrations of salt is consistent with the values measured by Gribbon *et al.* [11] using FRAP experiments, when the different sizes of the molecules are taken into account. In the latter study 500 kDa hyaluronan gave a diffusion coefficient of $D=7.9 \mu\text{m}^2/\text{s}$, while 830 kDa hyaluronan diffused with $D=5.6 \mu\text{m}^2/\text{s}$ in phosphate-buffered saline.

The single molecule approach used in our study was shown previously to yield accurate values for the diffusion coefficient of molecules in solution [12] and at the plasma membrane [17, 22]. In experiments at the single molecule level extremely low concentrations of fluorescent molecules can be analyzed (0.3 nM in our study). Thus, the diffusion coefficients obtained virtually represent the behavior of molecules at zero concentration. This is an important difference to measurements by a bulk technique like FRAP, which were used extensively in the past to study the transport of molecules at membranes [14] and in solution [11] at much higher than sub-nanomolar concentrations. As in other bulk methods, measurements at different concentrations and extrapolation to zero concentration were used in order to obtain information on the molecular conformation of individual hyaluronan molecules [11]. The estimation of diffusion coefficients at zero concentration from FRAP data involves a phenomenological extrapolation step based on the application of a universal scaling equation for polymer self-diffusion [19], which is not required in the analysis of single molecule trajectories.

The diffusion coefficient of a spherical molecule is related to its hydrodynamic radius according to the Stokes–Einstein equation $D=k_B T/6\pi\eta R_h$, where k_B is the Boltzmann constant, T the absolute temperature and η is the viscosity of the solvent. Since the images of single hyaluronan molecules in solution indicated that these form random coils (see above, Fig. 1) their global shape would be approximated by a sphere when the temporal fluctuations of these polymers were averaged. Therefore, we estimated the hydrodynamic radius R_h of hyaluronan from

rooster comb to be 72 nm in physiological saline buffered with tris. The radius, r , of a spherical molecule is related to its density, ρ , and mass, m , according to the equation $r=(3m/N_A 4\pi\rho)^{1/3}$ where N_A is the Avogadro constant. Thus, we calculate 1 g of 1,500 kDa hyaluronan to occupy a solvent volume of 0.847 l. This value is in excellent agreement with earlier reports [15]. Furthermore, the hydrodynamic radius determined in our study is consistent with the persistence length of hyaluronan which was reported to be 5 nm according to small-angle X-ray scattering and intrinsic viscosity measurements and 8.7 nm according to dynamic and total intensity light scattering (reviewed in [10]). The persistence length ξ_L is half of the Kuhn length l_K , *i.e.* the length of hypothetical segments that the chain can be considered as freely joined. When N_K denotes the effective number of repeat units, the radius of gyration R_g of a freely joined chain is related to l_K according to the equation $R_g=(N_K)^{1/2}l_K/6^{1/2}$ [1]. Assuming a contour length $L=4 \mu\text{m}$ ($=N_K \cdot l_K$) for hyaluronan of 1,500 kDa and estimating $R_g \approx R_h=72 \text{ nm}$ we calculate $N_K=514$ and $l_K \approx 8 \text{ nm}$. Thus, $\xi_L \approx 4 \text{ nm}$ in agreement with the result obtained from small-angle X-ray scattering and intrinsic viscosity measurements.

Taken together, our results show that real-time observation of individual hyaluronan molecules in aqueous solution is readily feasible. The quantitative analysis of the diffusion of hyaluronan using this approach directly leads to results, which are compatible with results from bulk methods published earlier. Moreover, our observations fully support the concept that single hyaluronan molecules form random coil structures with low density in solution. The possibility of examining single hyaluronan molecules in solution has important implications for future studies of the extracellular matrix. First, it sheds new light on how ordered hyaluronan structures form *e.g.* on surfaces *in vitro* as observed by EM [20] and AFM [5], or even *in vivo* [2, 8, 24]. On the other hand, the visualization of the interaction of cells with single hyaluronan molecules allows a completely new approach to the study of receptor binding, endocytosis and degradation events.

Acknowledgements We thank Hanns Häberlein, Rudolph Merkel, Martin Rost, Anne Sieben, Uwe Rauch and Roger Klein for very helpful discussions and suggestions, and Marc Hebest for providing chicken muscle actin. This study was supported by BMBF grant 01GN0502 to J.K and V.G. UK acknowledges financial support by the German Research Foundation (DFG grant Ku 1507/1-2).

References

1. Atkins, P.W.: Physical Chemistry, 4th edn. OUP, Oxford (1990)
2. Baier, C., Baader, S.L., Jankowski, J., Gieselmann, V., Schilling, K., Rauch, U., Kappler, J.: Hyaluronan is organized into fiber-like

- structures along migratory pathways in the developing mouse cerebellum. *Matrix Biol.* **26**, 348–358 (2007)
3. Bitter, T., Muir, H.M.: A modified uronic acid carbazole reaction. *Anal. Biochem.* **4**, 330–334 (1962)
 4. Cowman, M.K., Matsuoka, S.: Experimental approaches to hyaluronan structure. *Carbohydr. Res.* **340**, 791–809 (2005)
 5. Cowman, M.K., Spagnoli, C., Kudasheva, D., Li, M., Dyal, A., Kanai, S., Balazs, E.A.: Extended, relaxed, and condensed conformations of hyaluronan observed by atomic force microscopy. *Biophys. J.* **88**, 590–602 (2005)
 6. Crank, J.: *The Mathematics of Diffusion*. Clarendon, Oxford (1975)
 7. de Belder, A.N., Wik, K.O.: Preparation and properties of fluorescein-labelled hyaluronate. *Carbohydr. Res.* **44**, 251–257 (1975)
 8. de La Motte, C.A., Hascall, V.C., Calabro, A., Yen-Lieberman, B., Strong, S.A.: Mononuclear leukocytes preferentially bind via CD44 to hyaluronan on human intestinal mucosal smooth muscle cells after virus infection or treatment with poly(I.C). *J. Biol. Chem.* **274**, 30747–30755 (1999)
 9. de la Motte, C.A., Hascall, V.C., Drazba, J., Bandyopadhyay, S.K., Strong, S.A.: Mononuclear leukocytes bind to specific hyaluronan structures on colon mucosal smooth muscle cells treated with polyinosinic acid:polycytidylic acid: inter-alpha-trypsin inhibitor is crucial to structure and function. *Am. J. Pathol.* **163**, 121–133 (2003)
 10. Furlan, S., La Penna, G., Perico, A., Cesaro, A.: Hyaluronan chain conformation and dynamics. *Carbohydr. Res.* **340**, 959–970 (2005)
 11. Gribbon, P., Heng, B.C., Hardingham, T.E.: The molecular basis of the solution properties of hyaluronan investigated by confocal fluorescence recovery after photobleaching. *Biophys. J.* **77**, 2210–2216 (1999)
 12. Grünwald, D., Hoekstra, A., Dange, T., Buschmann, V., Kubitscheck, U.: Direct observation of single protein molecules in aqueous solution. *Chemphyschem* **7**, 812–815 (2006)
 13. Grünwald, D., Spottke, B., Buschmann, V., Kubitscheck, U.: Intranuclear binding kinetics and mobility of single native U1 snRNP particles in living cells. *Mol. Biol. Cell* **17**, 5017–5027 (2006)
 14. Kubitscheck, U., Wedekind, P., Peters, R.: Lateral diffusion measurement at high spatial resolution by scanning microphotolysis in a confocal microscope. *Biophys. J.* **67**, 948–956 (1994)
 15. Laurent, T.C., Fraser, J.R.: Hyaluronan. *Faseb. J.* **6**, 2397–2404 (1992)
 16. Lee, H.G., Cowman, M.K.: An agarose gel electrophoretic method for analysis of hyaluronan molecular weight distribution. *Anal. Biochem.* **219**, 278–287 (1994)
 17. Lommerse, P.H., Blab, G.A., Cognet, L., Harms, G.S., Snaar-Jagalska, B.E., Spaink, H.P., Schmidt, T.: Single-molecule imaging of the H-ras membrane-anchor reveals domains in the cytoplasmic leaflet of the cell membrane. *Biophys. J.* **86**, 609–616 (2004)
 18. McDonald, J., Hascall, V.C.: Hyaluronan minireview series. *J. Biol. Chem.* **277**, 4575–4579 (2002)
 19. Phillies, G.D.J.: The hydrodynamic scaling model for polymer self-diffusion. *J. Phys. Chem.* **93**, 5029–5039 (1989)
 20. Scott, J.E., Cummings, C., Brass, A., Chen, Y.: Secondary and tertiary structures of hyaluronan in aqueous solution, investigated by rotary shadowing-electron microscopy and computer simulation. Hyaluronan is a very efficient network-forming polymer. *Biochem. J.* **274**(Pt 3), 699–705 (1991)
 21. Siebrasse, J.P., Grünwald, D., Kubitscheck, U.: Single-molecule tracking in eukaryotic cell nuclei. *Anal. Bioanal. Chem.* **387**, 41–44 (2007)
 22. Sonnleitner, A., Schütz, G.J., Schmidt, T.: Free Brownian motion of individual lipid molecules in biomembranes. *Biophys. J.* **77**, 2638–2642 (1999)
 23. Stern, R., Asari, A.A., Sugahara, K.N.: Hyaluronan fragments: an information-rich system. *Eur. J. Cell Biol.* **85**, 699–715 (2006)
 24. Zhang, H., Baader, S.L., Sixt, M., Kappler, J., Rauch, U.: Neurocan-GFP fusion protein: a new approach to detect hyaluronan on tissue sections and living cells. *J. Histochem. Cytochem.* **52**, 915–922 (2004)